

APPROXIMATE ESTIMATION OF HARDENING-SOFTENING BEHAVIOUR OF CIRCULAR PIPES SUBJECTED TO PURE BENDING

Yang Jialing (杨嘉陵)

(The Solid Mechanics Research Centre, Beijing University of Aeronautics and Astronautics,
Beijing 100083, China)

S. R. Reid

(Department of Mechanical Engineering, UMIST, P.O.Box 88, Manchester M60 1QD, UK)

ABSTRACT: An approximate method for describing the plastic hardening-softening behaviour of circular pipes subjected to pure bending is presented. Theoretical estimation based on the uniform ovalization model and local collapse model proposed in the paper is incorporated to give several simple formulations with reasonable accuracy for determining the relationship between bending moment (M) and curvature (κ) in the purely bended pipes. Attention is focused on the critical curvature associated with maximum resistant moment and the maximum change in the original diameter before the end of uniform ovalization stage as well as the local collapse behaviour. Some comparisons between analytical results and experimental results are made in order to examine the theory.

KEY WORDS: hardening-softening behaviour, pure bended pipes, circular pipes, deformation characteristics of pipes

1 INTRODUCTION

The deformation characteristics of pipes subjected to bending moment are more complicated than that of the pipes subjected to uniform axial compression, although the latter attracts more studies than the former whose application is quite extensive in engineering such as power plant and offshore structural system. For those frequently used pipes with outer diameter (D) to thickness (H) ratio (D/H) between 15 to 40, according to the observation of the pure bending test and theoretical analysis published in the past, the deformation process of the bending pipe from initial elastic bending to large plastic local collapse can be described by three stages in the curve of its relationship between the bending moment and curvatures as shown in Fig.1, which is summarized in the following:

(1) Elastic bending stage of conforming to classical beam theory. The linear relations between the bending (M) and the curvature (κ) precisely conform the classical beam theory,

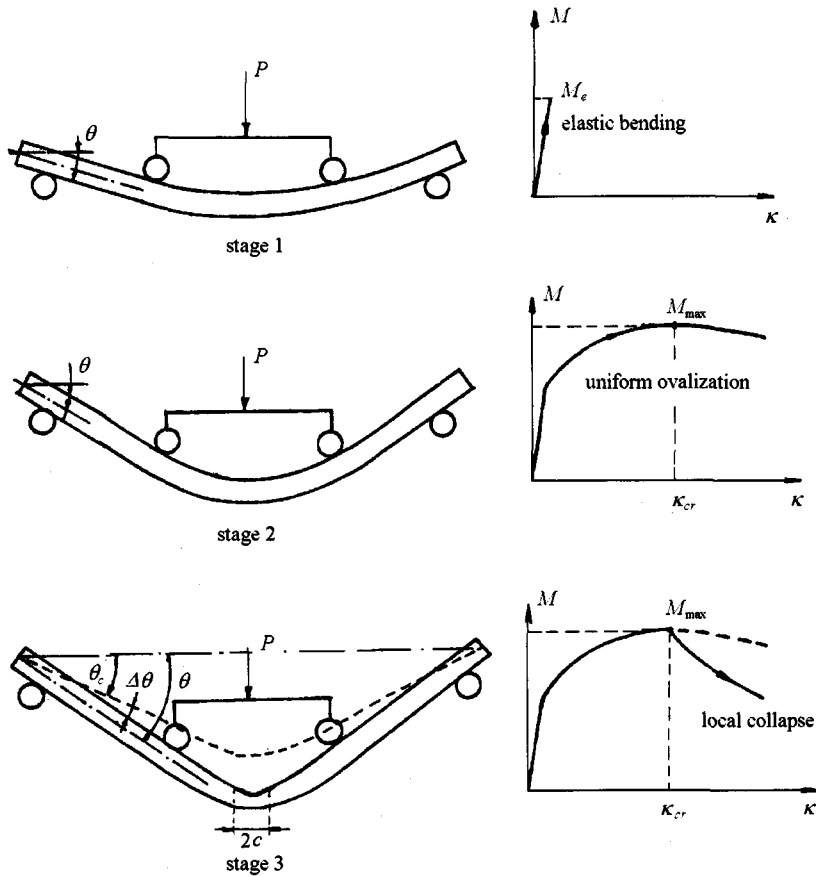


Fig.1 Deformation process of pure bending pipes and moment-curvature response

and the equation is given by

$$M = EI\kappa \tag{1}$$

where E is Young's modulus and I the second moment of area of the cross-section. No obvious ovalization of the pipe's cross-section can be observed and therefore the estimation based on classical beam theory is in good agreement with experimental results.

(2) Plastic hardening bending stage with uniform ovalized cross-section. With the increase of curvature, more and more materials of the cross-section enter into the plastic state from outer fibre toward the cross-section centre. The uniform ovalization of the cross-section becomes remarkable. For those pipes with $D/H = 15 \sim 40$, the ovalization is significantly influenced by the plastic behaviour of the material. During the initial stage of ovalization, the strain hardening still governs the resistant bending of the cross-section when comparing with the progressive reduction of bending rigidity of the pipe resulted from the ovalization. So the resistant bending moment increases with the growing of curvature. The development of the ovalization, however, will eventually overwhelm the effect of strain strength of the material and consequently a critical curvature is observed where the bending moment reaches its maximum value. Hereafter, further increase of the curvature results in a drop of bending moment which leads to local buckling and collapse of the pipe (see following stage 3). Therefore the research of the critical curvature (or strain) is important

in the evaluation of load carrying capacity of pipes. Since Brazier^[3] studied the problem in the range of elasticity in 1927, a series of studies by using plastic theory associated with numerical methods and pure bending tests have been carried out by several researchers^[4~10]. The key results can be summarized as a relationship between outer fibre critical strain (ϵ_c) corresponding to the critical curvature (κ_c) of the pure bending cross-section and the ratio of the thickness to outer diameter (H/D) of the pipes. The critical strain and curvature can be approximately expressed by

$$\epsilon_c = C \frac{H}{R} \qquad \kappa_c = C \frac{H}{R^2} \qquad (2)$$

where C is a constant and $R = D/2$. It is observed that most of the experimental data is in the narrow range between the lines defined by Eq.(2) with $C = 0.2$ and 0.5 . During the uniform ovalization stage, the cross-section of pipes is deformed to be like the shape of an ellipse. The ovalization rate characterized by the shortening of the pipe diameter is small in comparing with D , usually less than 10%. But this leads to critical transition of load carrying capacity from strengthening to weakening of the pipe.

(3) Local collapse stage with nonuniform ovalization. During the latter period of uniform ovalization when resistant bending is close to its maximum value, a series of short wavelength "ripples" become more visible on the compression side along the axial direction of the pipe, which is similar to the bifurcation buckling of an axially compressed shell. The uniform ovalization soon stops and the "ripples" localize into a "kink" while the bending moment drops sharply, leading to catastrophic collapse. Four point bending test shows that the "kink" is restricted in a small region (see Fig.2) whose half-length (c) can be estimated by $c = \beta(DH)^{0.5}$ where β is a constant depending on the property of the material while other regions are in the unloading state. As the serious localization of deformation occurs in the region of

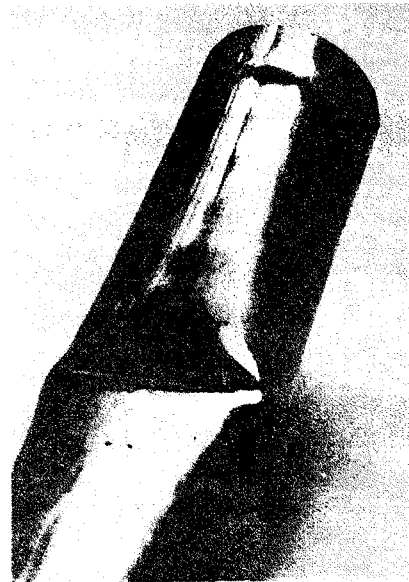


Fig.2 Local collapse characterized by a "kink"

the "kink", an abrupt change of the slope over the "kink" in pipe line direction can be observed, and therefore the relationship between bending moment (M) and the rotation (θ) of the "kink" are available to describe the local collapse behaviour of the pipe rather than using the moment-curvature relation. However, as a generalized constitutive characteristic study of the hardening-softening behaviour of pure bended pipes, it is desired to utilize the unified parameters (M - κ relation) for description of the deformation history of the three stages introduced above. By noting that the "kink" is formed also in a small region, the average curvature increment can be defined in this region by

$$\Delta\kappa = \Delta\theta/c \qquad (3)$$

and then the moment-curvature relationship during local collapse stage can be also depicted, which is sketched in Fig.1 of stage 3.

The precise theoretical elastic-plastic analysis of the local collapse behaviour of a pipe under pure bending is quite complicated, having to do with 3-D large deformation equation of the shell. As a rough estimation with reasonable accuracy, however, a simple model based on the plastic yield line method is proposed in the paper which achieves fairly good agreement with experimental results.

As to the application of the $M-\kappa$ relationship of pipes under pure bending, it is worthwhile to mention the pipe-whip model suggested by Reid et al.^[11]. The model, incorporating the generalized constitutive relationship between M and κ which takes account of the whole deformation history described in above three stages into large deflected dynamic governing equations based on beam theory, provides a good estimation of the dynamic behaviour of whipping pipes through a series comparisons between theoretical results and experiment data.

The objective of this paper is to suggest an approximate method for describing the elastic-plastic hardening-softening behaviour of pipes subjected to pure bending. Attention is focused on the simplification of the formulations based on [1] with reasonable accuracy to give the approximate description of the $M-\kappa$ relationship in uniform ovalization stage and suggest a new model to describe the local collapse behaviour of the bended pipe.

2 UNIFORM OVALIZATION BEHAVIOUR

2.1 Essential Formulation of the Problem From [1]

Figure 3 shows schematically the deformed shape of an infinitely long circular pipe subjected to pure bending. Three basic assumptions adopted in [1] for the analysis are as follows:

(1) the middle surface of the pipe is inextensible, which is based on experimental observation and this condition can be expressed by

$$w = dv/d\theta \quad (4)$$

where v and w are displacement components at middle surface in circumferential and radial direction, respectively. According to the geometric relations between strain and displacements, the longitudinal strain ε_X and circumferential bending strain ε_S can be expressed by

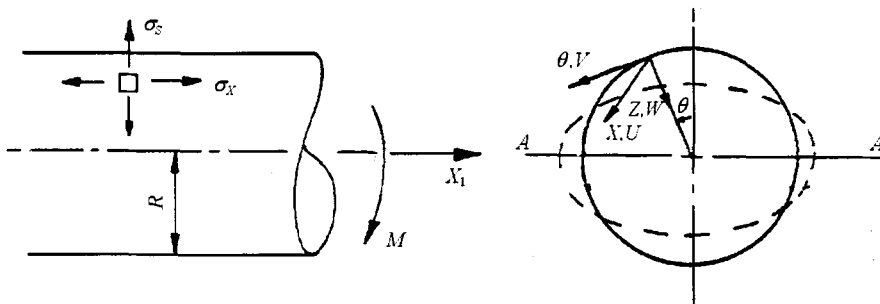


Fig.3 Middle surface of a pipe subjected to bending

$$\varepsilon_X = \kappa[(R - w) \cos \theta - v \sin \theta] \quad (5a)$$

$$\varepsilon_S = \frac{Z}{R^2} \left(w + \frac{\partial^2 w}{\partial \theta^2} \right) \quad (5b)$$

where θ is co-ordinate as shown in Fig.3

(2) the volume of the pipe element is incompressible during plastic deformation, and by employing the deformation theory of plasticity, the constitutive equations are given by

$$\sigma_X = \frac{2\bar{\sigma}}{3\bar{\varepsilon}}(2\varepsilon_X + \varepsilon_S) \quad (6a)$$

$$\sigma_S = \frac{2\bar{\sigma}}{3\bar{\varepsilon}}(2\varepsilon_S + \varepsilon_X) \quad (6b)$$

where $\bar{\varepsilon}$ and $\bar{\sigma}$ are the effective strain and stress, respectively.

(3) the plastic material behaviour is modeled by a power hardening law of the form

$$\bar{\sigma} = \sigma_0 \bar{\varepsilon}^n \quad (7)$$

where σ_0 and n are two characteristic constants of the material, obtained from a best fit to the experimental stress-strain curve. The effective strain $\bar{\varepsilon}$ is given by

$$\bar{\varepsilon} = \frac{2}{\sqrt{3}}(\varepsilon_S^2 + \varepsilon_X^2 + \varepsilon_S \varepsilon_X)^{0.5} \quad (8)$$

Based on above assumptions, the strain energy per unit length of the pipe is given by

$$U = \frac{4}{3}\sigma_0 \int_0^\pi R \int_{-H/2}^{H/2} \left[\int_0^{\varepsilon_X} \bar{\varepsilon}^{n-1}(2\varepsilon_X + \varepsilon_S) d\varepsilon_X + \int_0^{\varepsilon_S} \bar{\varepsilon}^{n-1}(2\varepsilon_S + \varepsilon_X) d\varepsilon_S \right] dZ d\theta \quad (9)$$

According to extremum and variational principles, the real stress and strain fields which satisfy the equilibrium equations in the bending pipe render the strain energy, U , minimum. The numerical calculation is carried out by letting the displacement, w , be expressed by a series of orthogonal functions

$$w = R \sum_{i=1}^{\infty} \zeta_i \tilde{\phi}_i(\theta) \quad (10)$$

where $\phi_1(\theta), \phi_2(\theta), \dots$ and $\phi_n(\theta)$ are the displacement functions which are normally chosen to satisfy

$$\left. \frac{d\tilde{\phi}_i}{d\theta} \right|_{\theta=0, \pi} = 0 \quad (11)$$

due to symmetry about the vertical plane of the cross-section. $\zeta_1, \zeta_2, \dots, \zeta_n$ can be determined by the stationary nature of U , and then the applied bending moment, M , is calculated by

$$M = \frac{\partial}{\partial \kappa}(U^{\min}) \quad (12)$$

2.2 Approximate Analysis

Although [1] suggested an approximate method for simplifying the numerical calculation, no further simple formulations were provided to estimate the M - κ relationship and

critical curvature and bending value. An extended and improved procedure is presented and some approximate estimate formulations with reasonable accuracy are given in the section.

After integration of Eq.(9) with respect to ε_X and ε_S , the strain energy is found to be

$$U = \frac{8\sigma_0 RH}{3(n+1)} \left(\frac{2}{\sqrt{3}}\right)^{n-1} \int_0^\pi \int_{-0.5}^{0.5} [2(\varepsilon_X^2 + \varepsilon_S^2 + \varepsilon_X \varepsilon_S)^{\frac{n+1}{2}} - |\varepsilon_X|^{n+1} - |\varepsilon_S|^{n+1}] dz d\theta \quad (13)$$

where $z = Z/H$. During uniform ovalization, pure bending experiment shows that the changes of the cross-section in vertical and horizontal diameters were quite close to each other, indicating that it is reasonable to assume that the pipe which is initially round becomes elliptical shape^[4], and therefore the strains ε_X and ε_S are expressed by functions of θ and z ,

$$\varepsilon_X = \frac{\kappa D}{2} f_1(\theta, \zeta) \quad \varepsilon_S = \frac{-6zH}{D} f_2(\theta, \zeta) \quad (14a, 14b)$$

where

$$f_1 = \cos \theta (1 - \zeta \cos^2 \theta) \quad f_2 = \zeta \cos 2\theta \quad (15a, 15b)$$

Introduce a characteristic curvature κ_0 which is defined by

$$\kappa_0 = \frac{H}{D^2} \quad (16)$$

and then ε_X is rewritten in the form

$$\varepsilon_X = \frac{H}{2D} \bar{\kappa} f_1(\theta, \zeta) \quad (17)$$

where $\bar{\kappa} = \kappa/\kappa_0$ is the nondimensional curvature. Using (14) and (17), the strain energy Eq.(13) can be rearranged as

$$U = \frac{4\sigma_0 DH}{3(n+1)} \left(\frac{2}{\sqrt{3}}\right)^n (H/D)^{n+1} \left\{ \int_0^\pi \int_{-1}^1 \left(\frac{\bar{\kappa}^2 f_1^2}{4} - \frac{3z\bar{\kappa}}{2} f_1 f_2 + 9z^2 f_2^2 \right)^{\frac{n+1}{2}} dz d\theta - \left(\frac{\bar{\kappa}}{2}\right)^{n+1} \int_0^\pi |f_1|^{n+1} d\theta - \frac{6 \times 3^n}{n+2} \int_0^\pi |f_2|^{n+1} d\theta \right\} \quad (18)$$

In the first double integral, the integration from the lower-limit -1 to the upper limit 1 , can be approximated by a Gauss three-point integral formulation and after setting $\theta = \pi/2 - \phi$, above equation becomes

$$U \approx \frac{2\sigma_0 DH}{3(n+1)} \left(\frac{2}{\sqrt{3}}\right)^{n-1} (H/D)^{n+1} U^* \quad (19)$$

in which

$$U^* = \int_{-\pi/2}^{\pi/2} 2.22 [0.25\bar{\kappa}^2 f_1^2 - 1.1619\bar{\kappa} f_1 f_2 + 5.4f_2^2]^{\frac{n+1}{2}} d\phi - 0.448 \left(\frac{\bar{\kappa}}{2}\right)^{n+1} \int_0^{\pi/2} |f_1|^{n+1} d\phi - \frac{12 \times 3^n}{n+2} \int_0^{\pi/2} |f_2|^{n+1} d\phi \quad (20)$$

where

$$f_1 = \sin \phi (1 - \zeta \sin^2 \phi) \quad f_2 = \zeta (2 \sin^2 \phi - 1) \quad (21)$$

The above integral can be easily estimated by Simpson's method and the minimum U^* , therefore, is determined by a given $\bar{\kappa}$ with an appropriate value of ζ which renders the integral minimum. The bending-curvature relationship is obtained by

$$M = \frac{\partial U^{\min}}{\partial \kappa} = \frac{\sigma_0 D^2 H}{2(n+1)} \left(\frac{2}{\sqrt{3}}\right)^{n+1} (H/D)^n M^* \tag{22}$$

where

$$M^* = \frac{\partial U^{*\min}}{\partial \bar{\kappa}} \tag{23}$$

depending on both $\bar{\kappa}$ and material strain hardening exponent n , and the critical non-dimensional curvature $\bar{\kappa}_c$ is attained by setting

$$\left\{ \frac{\partial M^*}{\partial \bar{\kappa}} \right\}_{\bar{\kappa}=\bar{\kappa}_c} = 0 \tag{24}$$

for which, the bending moment reaches its maximum values.

2.3 Approximate Formulation and Comparison

Equation (24) indicates that $\bar{\kappa}_c$ only depends on the material strain hardening exponent n . For those experimental stress-strain curves whose plastic behaviour can be approximately described by power law formulation (7), n is usually in the range of $0.15 < n < 0.3$ for materials such as low carbon steel and aluminum, and $0.35 < n < 0.5$ for hardening materials such as alloyed structural steel. As a typical example, n is selected to be 0.26, a representative hardening exponent for mild steel. From (22) and (20), it is found that

$$M^* \approx -0.218\bar{\kappa}^2 + 0.5105\bar{\kappa} + 1.242 \tag{25}$$

for $0.35 \leq \bar{\kappa} \leq 2.0$ and hence from (24), it is estimated that

$$\bar{\kappa}_c = 1.2 \tag{26}$$

which gives

$$\kappa_c \approx 0.3 \frac{H}{R^2} \tag{27}$$

The difference between the result and that from Reid et al.^[1] when letting $R = 24.1$ mm and $H = 2.6$ mm is less than 4%.

For $0.15 < n < 0.5$, (22) together with (20) provides a good approximate estimate formulation for $\bar{\kappa}_c$ and M_{\max}^* which are

$$\bar{\kappa}_c \approx n^{0.8-n}(2.65 - n) \tag{28a}$$

$$M_{\max}^* \approx 1.478 + n^2 \tag{28b}$$

The critical curvature κ_c as well as the critical strain ε_c are then approximately estimated by

$$\kappa_c \approx \frac{1}{4} n^{0.8-n}(2.65 - n) \frac{H}{R^2} \tag{29a}$$

$$\varepsilon_c \approx \frac{1}{4} n^{0.8-n}(2.65 - n) \frac{H}{R} \tag{29b}$$

Comparing with Eq.(2), it is estimated that the value of C varies between 0.18 and 0.43 for the materials with n varying from 0.15 to 0.5. In order to further examine Eq.(29), a comparison with the experimental results given by Reddy^[2] is made herein. Figure 4 shows two typical actual stress-strain curves for steel and aluminum alloy specimens which are given by Reddy^[2]. The curves can be approximated by

$$\sigma = 5784\epsilon^{0.39} \quad \text{for the steel} \tag{30a}$$

$$\sigma = 998\epsilon^{0.2} \quad \text{for the aluminum} \tag{30b}$$

to describe their plastic behaviour. After putting $n = 0.39$ and $n = 0.2$ into Eq.(29), it gives

$$\left. \begin{aligned} \epsilon_c &= 0.38 \frac{H}{R} && \text{for steel pipes} \\ \epsilon_c &= 0.23 \frac{H}{R} && \text{for aluminum pipes} \end{aligned} \right\} \tag{31}$$

These estimations provides excellent agreement with the experiment results for both steel and alloy aluminum pipes which are shown in Fig.5 plotted by Reddy^[2].

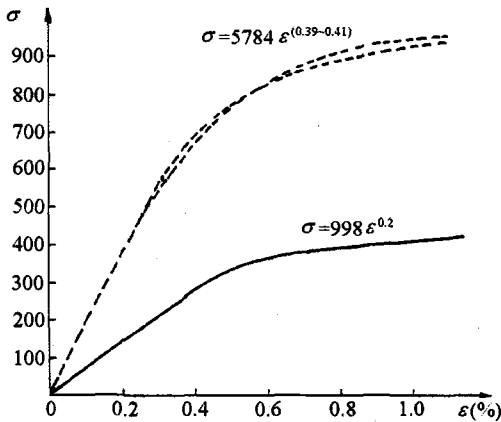


Fig.4 Stress-strain curves of materials used in Reddy's test

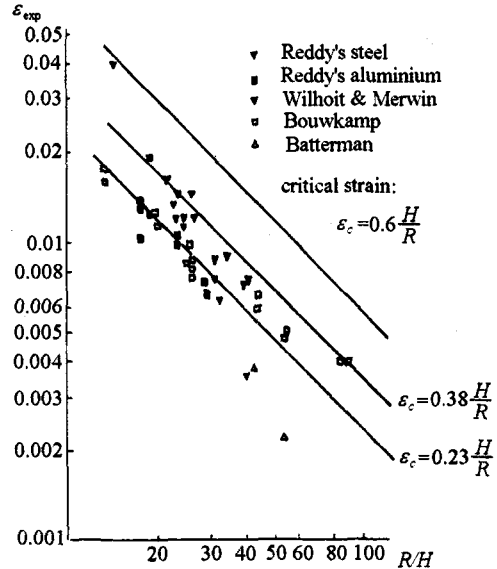


Fig.5 Comparisons between theoretical predictions and experimental data

On the other hand, the maximum bending moment can be approximately estimated by substituting (28b) into (22), which gives

$$M_{\max} = \left. \frac{\partial U^{\min}}{\partial \kappa} \right|_{\kappa=\kappa_c} \approx \frac{\sigma_0 D^2 H}{2(n+1)} \left(\frac{2}{\sqrt{3}} \right)^{n+1} \left(\frac{H}{D} \right)^n (1.478 + n^2) \tag{32}$$

The value of M_{\max} is always smaller than the value of M_{cb} estimated by the classical beam theory at the same point when $\kappa = \kappa_c$. But the difference between them is small as well because the flatten rate of the cross-section is very limited during the uniform ovalization stage. Based on classical beam theory, the value of M_{cb} can be estimated by

$$M_{cb} = 4 \int_0^{\pi/2} \sigma H R^2 \sin \theta d\theta = \frac{\sigma_0 D^2 H}{2^n} (H/D)^n \bar{\kappa}_c^n \int_0^{\pi/2} \sin^{n+1} \theta d\theta \tag{33}$$

and from (32) and (33), the ratio, r^* , of M_{\max} to M_{cb} is given by

$$r^* = \frac{M_{\max}}{M_{cb}} = \left(\frac{4}{\sqrt{3}}\right)^n \frac{1.478 + n^2}{\sqrt{3}(n+1)n^{n(n-0.8)}(2.65-n)^n I(n+1)} \quad (34)$$

where

$$I(n+1) \approx \frac{\pi}{4} \{0.889(0.5)^{\frac{n+1}{2}} + 0.5556[0.984^{n+1} + 0.176^{n+1}]\} \quad (35)$$

for the value of n varying between 0.15 and 0.5, it is found that r^* varies from 0.94 to 0.88 about 6% ~ 12% below the value obtained from the classical beam theory.

The maximum change, 2Δ , of the diameter in deformed cross-section at the end of the uniform ovalization when $\kappa = \bar{\kappa}_c$ ($M = M_{\max}$) can be roughly estimated by employing the classical beam theory (CBT) with taking into account of the ovalization. Assume that the vertical diameter decreases to $D - 2\Delta$ and horizontal diameter increases to $D + 2\Delta$ at the critical point when $\kappa = \bar{\kappa}_c$ and $M = M_{\max}$. Then for the oval shaped cross-section, CBT predicts its value of the bending moment, M_{oval} , thus

$$M_{\text{oval}} \approx \frac{\sigma_0 H D^2 \bar{\kappa}_c^n}{2^n} (H/D)^n \left\{1 - n \frac{\Delta}{R}\right\} \int_0^{\pi/2} \sin^{n+1} \theta \left\{1 - 2 \frac{\Delta}{R} \sin^2 \theta\right\} d\theta \quad (36)$$

At critical point where the bending moment reaches the maximum value, let (36) equal to (32) and neglect the high order term in Δ/R , the maximum change of the diameter then is approximately estimated by

$$\frac{\Delta}{R} \approx \frac{I(n+1) - \frac{2^{n-1}(2/\sqrt{3})^{n+1}(n^2 + 1.478)}{(n+1)n^{n(n-0.8)}(2.65-n)^n}}{2I(n+3) + nI(n+1)} \quad (37)$$

The maximum change of the diameter estimated from (37) is found to be in the range from 3.5% ~ 6.5% for n varying between 0.15 to 0.5, which is in quite good agreement with the observations by Reddy^[2] in his pure bending experiment.

2.4 Discussion

(1) It should be emphasized that all of the simple approximate formulations for estimation of critical curvature (κ_c) or strain (ϵ_c), maximum bending moment (M_{\max}) and the maximum change of diameter (Δ) are based on the plastic deformation theory associated with the effective strain-stress relationship obeying the hardening power-law form given in (7), (8). As is well known that this constitutive relation is better in describing the plastic behaviour of material, in particular, when the strain is larger, rather than elastic behaviour of material. The formulations presented in the paper, therefore, is appropriate for the case of D/H being smaller rather than for very thin shell. As mentioned before, the objective of the paper is to provide some approximate formulations for describing the M - κ behaviour for pipe-whip model, the background of the study is concerned with behaviour of pipes in nuclear power-plant where the actual used pipes having the ratio of D/H in the range of 15~40.

(2) To estimate the critical values of κ_c , ϵ_c , M_{\max} and Δ as accurately as possible, it is important to correctly determine the strain hardening exponent, n , which depends on the hardening plastic behaviour of the material. A suggested method is that (i) roughly estimate the upper plastic limit strain as $0.4H/R$; (ii) restrict the range of the stress-strain

curve experimentally obtained between the yield strain and the upper plastic limit strain, and fit the curve in the range with appropriate n and σ_0 in the form of (7); (iii) use (29) to estimate the critical strain defined here by ε_{c1} and check it to see if it is far smaller than $0.4H/D$. If it does, decrease the upper plastic limit strain to be slightly larger than ε_{c1} but close to it and then repeat (ii). If the newly obtained ε_{c2} is obviously larger than ε_{c1} , then select ε_{c2} as the new upper plastic limit strain and repeat (ii) step by step until satisfactory results is achieved.

(3) Recently, Calladine^[8] provided a simple estimate of the critical strain

$$\varepsilon_c \approx 0.7 \left(\frac{H}{R} \right) \left(\frac{E_t}{E_s} \right)^{0.5} \quad (38)$$

where E_s and E_t are the secant and tangent module, respectively, of the material. If the material is assumed to obey the power law relationship between stress and plastic strain as shown in Eq.(7) and noting $E_t = d\sigma/d\varepsilon$, $E_s = \sigma/\varepsilon$, then above equation becomes

$$\varepsilon_c \approx 0.7(H/R)\sqrt{n} \quad (39)$$

After putting $n = 0.39$ and $n = 0.2$ into Eq.(39) for the comparison with experimental result^[2], it gives

$$\left. \begin{aligned} \varepsilon_c &= 0.437 \frac{H}{R} && \text{for the steel pipe} \\ \varepsilon_c &= 0.313 \frac{H}{R} && \text{for the aluminum pipe} \end{aligned} \right\} \quad (40)$$

which are 15% and 36% larger than the estimations from Eq.(31).

3 LOCAL COLLAPSE BEHAVIOUR

3.1 Local Collapse Model

Four point bending tests performed on pipes have indicated that for pipes with D/H in the range of 15~40, the local collapse occurs shortly after the ripples have developed, see Fig.2. The plastic "kink" which is formed on the compression side of the pipe and initially localized in the range of a full wavelength of the ripple has the inverted triangular shape across the diameter as shown in Fig.6. The main yield plastic hinge line AC will deepen transversely into the pipe and grow along the circumferential direction. The nonuniform ovalized cross-section cut along the main hinge line is assumed to be deformed as shown in Fig.7 in which the initial change of the diameter during uniform ovalization stage is ignored since it is sufficient small. The resistant bending moment of the cross-section is contributed by the main hinge line (AC) and the rest flattening portion ABC . Based on the assumption that the circumferential middle surface of the pipe is inextensible, the geometrical relation for the deformed cross-section requires (Fig.7)

$$R_1 \sin \phi_1 = R\phi_0 \quad (41a)$$

$$(\pi - \phi_1)R_1 = (\pi - \phi_0)R \quad (41b)$$

where ϕ_0 , ϕ_1 and R_1 are defined in Fig.7. From above equation, ϕ_1 and R_1 can be expressed by

$$\phi_1 \approx 2.6264\phi_0^5 - 8.3378\phi_0^4 + 9.3784\phi_0^3 - 4.0942\phi_0^2 + 1.6181\phi_0 \quad (42a)$$

$$R_1 = \frac{(\pi - \phi_0)R}{\pi - \phi_1} \tag{42b}$$

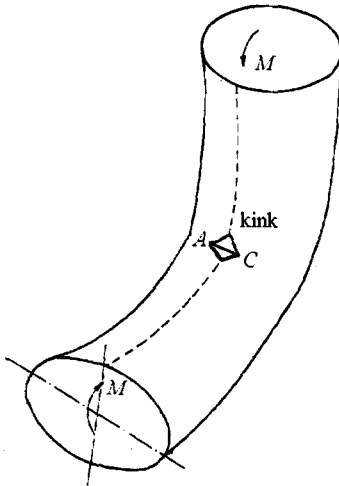


Fig.6 Position of "kink" in a bending pipe

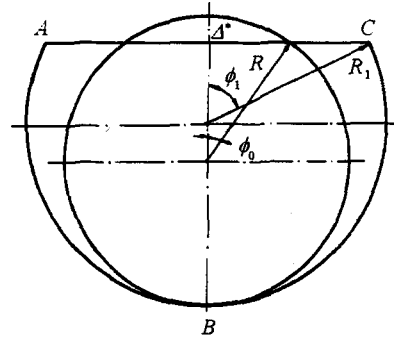


Fig.7 A cross-section of the "kink"

According to the pure bending test, the maximum moment M_{max} which occurs at the end of the uniform ovalization as described in section 2 is quite close to M_p , the fully plastic limit moment. This indicates that as first order estimate, it is reasonable to assume that the average axial stress, σ^* , of the ovalized cross-section during local collapse stage can be estimated by

$$\sigma^* \approx \frac{M_{max}}{4HR^2} \tag{43}$$

and therefore, the resistant bending moment contributed by the main hinge line AC can be obtained by

$$M_H^{AC} = \frac{1}{4}H^2\sigma^*D\phi_0 \tag{44}$$

while for the rest flattening portion of the cross-section (ABC), considering the equilibrium of the stress, the neutral axis position is determined by

$$\int_{A_1} \sigma dA_1 + \int_{A_2} \sigma dA_2 = 0 \tag{45}$$

where A_1 and A_2 are tension and compression stress regions divided by the neutral axis in the cross-section. It is found that the angle between the neutral axis and deformed circle centre is

$$\beta = \frac{\phi_1}{2} \tag{46}$$

The bending moment contributed by the flattening portion of the cross-section (ABC) is given by

$$M_{ABC} = 4\sigma^*R_1^2H \left(\cos \frac{\phi_1}{2} - \sin \phi_1 \right) \tag{47}$$

and the total resistant bending moment then is given by

$$M = M_H^{AC} + M_{ABC} = \frac{1}{4}\sigma^*H^2D\phi_0 + 4\sigma^*R_1^2H \left(\cos \frac{\phi_1}{2} - \frac{1}{2} \sin \phi_1 \right) \tag{48}$$

The longitudinal central section of the “kink” is shown in Fig.8 where ψ is an angle in relative to the uniform ovalized region of the pipe and x_1 and x_2 are defined in Fig.8. By considering the geometric relation, we have

$$x_1 = \sqrt{D \sin \frac{\psi}{2} \left(2c - D \sin \frac{\psi}{2} \right)} \tag{49a}$$

$$x_2 = D \cos \frac{\psi}{2} - \sqrt{D \sin \frac{\psi}{2} \left(2c - D \sin \frac{\psi}{2} \right)} \tag{49b}$$

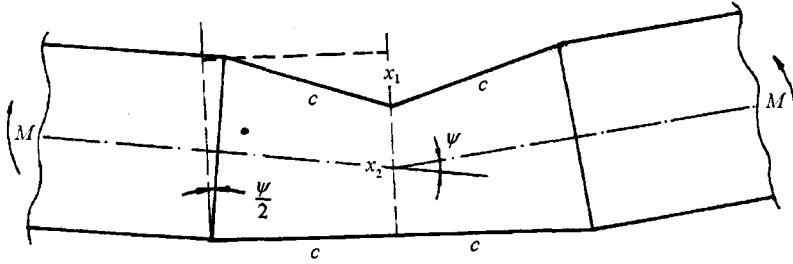


Fig.8 Deformation mechanism of the “kink”

and the change of the diameter is then estimated by

$$\Delta^* = D - x_2 \tag{50}$$

Therefore, from Fig.7 the relation between ϕ_0 and ψ is determined by

$$\phi_0 = \cos^{-1} \left\{ 1 - \frac{\Delta^*}{R} \right\} = \cos^{-1} \left\{ 1 - 2 \left[1 - \cos \frac{\psi}{2} + \sqrt{\sin \frac{\psi}{2} \left(\frac{c}{R} - \sin \frac{\psi}{2} \right)} \right] \right\} \tag{51}$$

Finally, the resistant bending moment in the localized cross-section is obtained by substitution of (42) into (48), thus

$$M = M_{\max} \left\{ \left[\frac{\pi - \phi_0}{\pi - \phi_1} \right] \left[\cos \frac{\phi_1}{2} - \frac{1}{2} \sin \phi_1 \right] + \frac{1}{8} \phi_0 \frac{H}{R} \right\} \tag{52}$$

As mentioned before, the “kink” is restricted in a small region and its half-length c can be written in the form

$$c = \lambda \sqrt{DH} \tag{53}$$

where λ is a constant depending on the property of the material. At initiation of local collapse stage, Murry and Bilston^[12] found that the half length of ripples which is measured from both their axial compression and bending test can be perfectly estimated by

$$c \approx \frac{\pi \sqrt{HR}}{[12(1 - \nu^2)]^{0.25}} \approx 1.22 \sqrt{DH} \tag{54}$$

where ν is Poisson’s ratio. This value is assumed to be the approximate half-length of the “kink” and, therefore the curvature corresponding to the bending moment from Eq.(54) during local collapse stage can be estimated by

$$\kappa = \kappa_c + \frac{\psi}{2c} \tag{55}$$

in the region of the “kink”. When $\psi = 0$, Eqs.(55) and (52) give

$$\kappa = \kappa_c \qquad M = M_{\max} \qquad (56)$$

since $\phi_0 = \phi_1 = 0$. This is the critical point between the uniform ovalization and local collapse stages.

3.2 Examples

In the previous section it is suggested that the bending moment and curvature relationship during local collapse stage should be approximately estimated from (52) and (55). When the structural parameters D, H and the material property E, σ_0 and n of the pipe are given, the behaviour of the pipe from elastic bending stage to uniform ovalization until local collapse can be estimated following the description in above. As the examples, Fig.9 shows three typical $M-\kappa$ relationship curves for mild steel pipes ($E = 200 \text{ GN/m}^2$, $\sigma_0 = 830 \text{ MN/m}^2$, $n = 0.26$) which are used in pipe-whip tests. Each of the three pipes has the same outer diameter 50.8 mm with wall-thickness of $H = 2.6 \text{ mm}$, 1.8 mm and 1.58 mm , respectively. It is seen that the values of the critical points (M_{\max}, κ_c) estimated from (32) and (30) are (1720 Nm, 1.34 m), (1120 Nm, 0.90 m) and (960 Nm, 0.8 m), respectively, for 2.6 mm, 1.8 mm and 1.58 mm wall-thickness pipes. After critical point, the pipes enter into the local collapse stage and the curve obviously departs from the uniform ovalization curves (Fig.9).

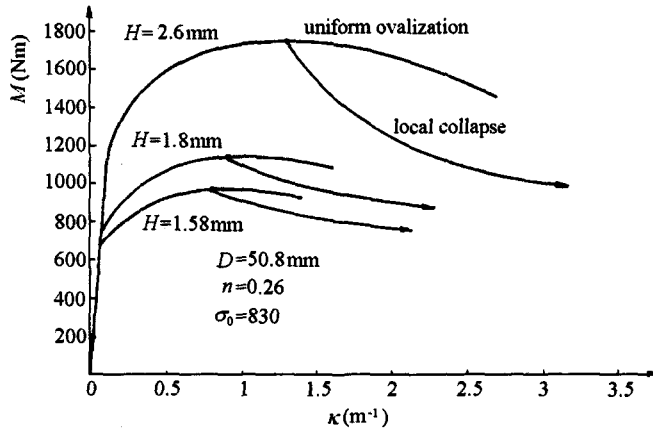


Fig.9 Moment-curvature relationship for three typical pipes

4 CONCLUSIONS

An approximate method was developed for the evaluation of the plastic hardening-softening behaviour i.e., the relationship between the bending moment and the curvature of pipes subjected to pure bending. Theoretical predictions from the simple analytical expressions suggested in this paper give results of the critical curvature, the critical strain, the maximum bending moment and the maximum change of the pipe diameter, which are in good agreement with the experimental ones during uniform ovalization. Based on observations of four-point bending tests, a local collapse model following the end of uniform ovalization stage was proposed to describe the softening behaviour of purely bended pipes. The formulations established are better applied to the pipes with D/H ranging 15 ~ 40.

REFERENCES

- 1 Reid SR, Yu TX, Yang JL. Hardening-softening behaviour of circular pipes under bending and tension. *Int J Mech Sci*, 1994, 36: 1073~1085
- 2 Reddy BD. An experimental study of the plastic buckling of circular cylinders in pure bending. *Int J Solids Structure*, 1979, 15: 669~683
- 3 Brazier LG. On the flexure of thin cylindrical shells and other sections. Proc R Soc Series A CXVI, 1926.104~114
- 4 Ades CS. Bending strength of tubing in the plastic range. *J Aero Sci*, 1957, 24: 505~510
- 5 Seide P, Weingarte VI. On the buckling of circular cylindrical shells under pure bending. *J Appl Mech ASME*, 1961, 28: 112~116
- 6 Akselrad EL. Refinement of the upper critical loading of pipe bending taking account of the geometric nonlinearity (In Russian) Izveatia. AN, SSR, OTN, Mekhanika, Machinostroenic, 1965, 4: 123~129
- 7 Gellin S. The plastic buckling of long cylindrical shells under pure bending. *Int J Solids Structures*, 1980, 16: 397~407
- 8 Calladine CR. Plastic buckling of tubes in pure bending. In: Thomson JMT, Hunt GM eds.: Collapse: The Buckling of Structure in Theory and Practice. Cambridge: Cambridge University Press, 1983. 111~124
- 9 Kyriakides S, Ju GT. Bifurcation and localization instabilities in cylindrical shells under pure bending—I. Experiments. *Int J Solids Structures*, 1992, 29: 1117~1142
- 10 Ju GT, Kyriakides S. Bifurcation and localization instabilities in cylindrical shells under pure bending—II. Predictions. *Int J Solids Structures*, 1992, 29: 1142~1171
- 11 Reid SR, Yu TX, Yang JL. Response of an elastic, plastic tubular cantilever beam subjected to force pulse at its tip—Small deflection analysis. *Int J Solids Structures*, 1995, 23: 3407~3421
- 12 Murry NW, Bilston P. Local buckling of thin-walled pipe being bent in the plastic range. *Thin-walled Structures*, 1992(14): 411~434